Study of ADI (After Develop Inspection) On Photo Resist Wafers Using Electron Beam (II)

Teruyuki Hayashi [a], Misako Saito[a], Kaoru Fujihara [a],Setsuko Shibuya [a],Y.Kudou[a],Hiroshi Nagaike [b]
Joseph Lin [c],Jack Jau [c]
[a] Tokyo Electron Ltd., 650 Mitsuzawa, Hosaka-cho, Nirasaki City, Yamanashi, Japan;
[b] Tokyo Electron AT Ltd., 2381-1 Kitashimojyo,Fujii-cho, Nirasaki City, Yamanashi, Japan;
[c] Hermes Microvision Inc.,1595 McCandless Drive Milpitas,CA USA95035

ABSTRACT

We have clarified that the low-damage, high-resolution defect inspection of the photo resist patterns is ensured by the electron-beam defect inspection equipment for 32-nm generation and beyond.
It has first been confirmed that the CD variations on the 65-nm width line structure formed on an ArF resist under general inspection conditions are equal to or less than the CD variations due to a general CD-SEM.
We have also succeeded in understanding the resist deterioration mechanism when the ArF resist is exposed to e-beams. This understanding has led us to learn that the layer that, located in the vicinity of the resist surface, is deteriorated by e-beams has its etching rate lowered to cause even improvement on the etching resistance.
These findings have enabled us to use inspection conditions that cause lower damage to resists. By using those conditions, we have been able to inspect ArF resist line-space structure wafers with line width of 65nm and pitch width of 140nm. The inspection successfully detected 15 to 20nm programmed extrusion defects with a capture rate of at least 95% and a nuisance rate of 5% or less.
It has thus been revealed that e-beam defect inspection equipment are useful for inspecting defects on resist wafers with 32-nm generation and beyond.

Keywords: inspection, photo resist, electron beam

1. INTRODUCTION

According to the International Technology Roadmap for Semiconductors (ITRS), it is reported that the defect size that needs to be controlled at the technology node of the hp 32-nm generation is 16 nm. In this generation, optical defect inspection equipment, which is currently in the mainstream, are believed to find difficulty in detecting such minute defects. As an alternative method, electron-beam defect inspection, which features better resolutions, is being studied [1)-3)]. In the previous report, we reported that e-beam inspection can detect minute defects of about 40-nm on the space area of a patterned wafer with a resist grating structure [4)]. On the other hand, however, it is known that the exposure to electron beam may cause resist damage [5)-8)]. For example, the resist damages are shrinkage and the elimination of the protective groups that are added to improve the etching resistance. Since the current used for an e-beam defect inspection equipment is generally over 1000 times higher than the current that flows in a CD-SEM, a concern is on damage to the resist as incurred by electron beams from defect inspection equipment.
We therefore decided to obtain an understanding of how an e-beam defect inspection equipment would give e-beam damage to ArF resists by evaluating the variation of the resist CD. We also studied the mechanism underlying the resist deterioration using Time-0f-Flight Secondary Ion Mass Spectrometry (TOF-SIMS), Fourier Transform Infrared Spectrometry (FTIR), Atomic Force Microscopy (AFM), and Gas Chromatography Mass Spectrometry (GC-MS). In addition, we evaluated the etching resistance of the e-beam exposed area. The findings obtained from these studies enabled us to set inspection conditions that would cause low damage to the resist.
It has been revealed that if such low-damage inspection conditions are used, defects of about 15 nm can be detected with high detection efficiency.
The above method has demonstrated that e-beam defect inspection equipment is a useful tool for detecting defects on patterned resist wafers of the 32-nm or later generation.

2. UNDERSTANDING THE BEHAVIOR OF RESIST PATTERN CD VARIATIONS CAUSED BY E-BEAM DEFECT INSPECTION TOOL

The sample was an Si wafer that was coated with a thermal oxidation film and a poly-Si film and was subjected to the application of Bottom Anti-Reflection Coating (BARC) and ArF resist to form a 65-nm line structure. Using the e-beam defect inspection equipment, e-beam was emitted onto the surface of this sample. A CD-SEM was used for CD measurement. The CD-SEM measurement condition was represented by 500 eV and 5 pA. The CD measurement procedure began with sample measurement with the CD-SEM, proceeded to e-beam exposure with the e-beam defect inspection equipment, and ended with sample measurement with the CD-SEM. The difference between the first and the second CD measurements was considered as CD variation. Therefore, the CD variation used here includes the resist CD change caused by the first CD-SEM observation.

First, the landing energy of the e-beam defect inspection equipment was varied. The results are shown in Figure 1. This figure indicates that the resist line width tends to slim slightly as the landing energy increases. The data plotted at a landing energy of 0 eV represents the result of only two CD measurements with the CD-SEM without e-beam exposure with the e-beam defect inspection equipment. This suggests that the first CD-SEM measurement caused the resist line width to shrink about 2%. It has been revealed that, under the experimental conditions used this time, the CD variations caused by the first CD-SEM measurement and e-beam exposure with the e-beam defect inspection equipment are 1% or lower in the region below 1800 eV except at 800 eV. These findings lead us to conclude that the CD variations caused by the e-beam defect inspection equipment are equal to or less than those caused by CD-SEM measurements in the region below 1800 eV except at 800 eV.

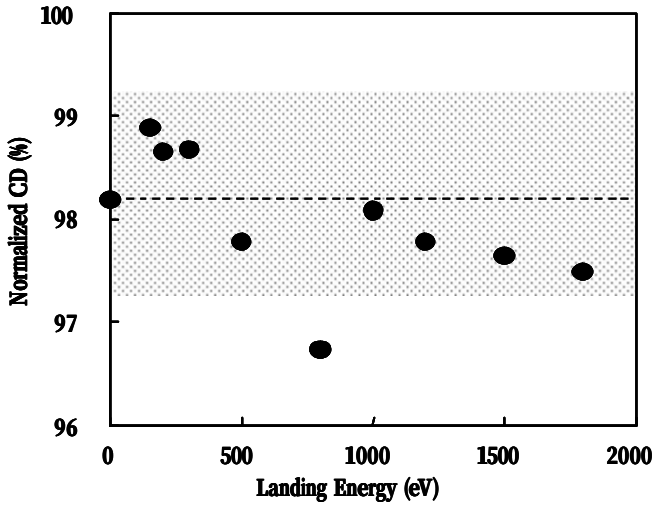

Fig.1 The CD variation depend on the landing energy of e-beam defect inspection. CD measurement procedure began with sample measurement with the CD-SEM, proceeded to e-beam exposure with the e-beam defect inspection equipment, and ended with sample measurement with the CD-SEM. The difference between the first and the second CD measurements was considered as CD variation. The data plotted at a landing energy of 0 eV represents the result of only two CD measurements with the CD-SEM without e-beam exposure with the e-beam defect inspection equipment.

Next, the number of scan averages for the e-beam defect inspection equipment was varied. Varying the number of scan averages varies the incident current to a unit area of the resist surface. The results are shown in Figure 2. The landing energy of the e-beam defect inspection equipment was set at 1500 eV. Under this condition, it has been revealed that the resist line width expand by increasing the number of scan averages. When the number of scan averages was equal to or greater than 16, the resist line width was considerably wider than the original resist line.

When the number of scan averages was 64, the resist line width was increased by no less than 30% compared with the original width.
The above findings lead us to conclude that the resist CD variations caused by e-beam exposure with an e-beam defect inspection equipment are comparable to or less than those caused by a general CD-SEM if the landing energy is below 1800 eV and the number of scan averages is up to 16.

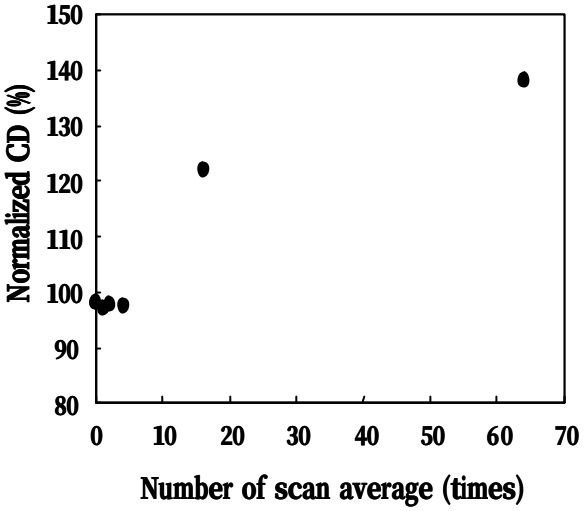

Fig.2 The CD variation depend on the number of scan average of the e-beam defect inspection.

3. UNDERSTANDING THE RESIST DETERIORATION MECHANISM IN E-BEAM DEFECT INSPECTION TOOL

One of the concerns regarding resist pattern inspection with an e-beam defect inspection equipment is resist deterioration caused by e-beam exposure. We therefore decided to study how the resist deterioration mechanism (which causes considerable CD variations) works and how deteriorated resists influence the etching resistance of the resist.
The sample was an Si wafer that was subjected to the application of BARC and an acrylic ArF resist and was not patterned. Using an e-beam defect inspection equipment, e-beam was emitted onto the resist surface. The e-beam exposure conditions were represented by a landing energy of 1500 eV and a scan averaging number of 16. As shown in Figure 3, a cut was made from the resist surface to the substrate at a shallow angle and that cut surface was measured at multiple points using TOF-SIMS and FTIR in order to evaluate the variations of the composition in the depth direction. The analysis based on the TOF-SIMS and FTIR observations has revealed that the acrylic ArF resist used this time contained an adamantane and a C=O bond that comes from a cycric ester. This indicates that the resist is a structure with an adamantyl group and lactone contained in side chains. We decided to evaluate the 2-methyl 2-adamantyl group using TOF-SIMS and the lactone using FTIR, as shown in Figure 4.
Figures 5 and 6 show the depth distributions of the respective side chains in the resist as observed using TOF-SIMS and FTIR. These figures indicate that both side chains are eliminated at a depth of about 60 to 70 nm from the resist surface by e-beam exposure. This depth matches the primary electron penetration depth obtained by a Monte Carlo Simulation (Figure 7).
Figure 8 shows the result of measuring the mass of the gas emitted from the resist which was placed in the ionization chamber of a GC-MS by exposure to e-beams with an energy of several tens of electron volts. This figure also indicates the detection of a mass that is due to the 2-methyl adamantyl group, which is the protective group in the resist used this time. This finding enables us to conclude that the side chains eliminated from the resist base by e-beam exposure was evaporated into vacuum.
It has thus been revealed that resist exposure to e-beam causes the side chains to be eliminated from the resist at the depth that can be reached by the incident primary electrons and to be evaporated, thereby giving rise to certain

deformation of the resist itself. The 2-methyl adamantyl group, which is included in the side changes that are eliminated and evaporated from the resist by e-beam exposure, is able to improve the etching resistance of the resist (to server as a protective group). Since the number of protective groups is reduced at a depth of about 60 to 70 nm from the resist surface, it is expected that the etching resistance is deteriorated near the resist surface due to e-beam exposure.

For further investigation, we assessed the difference between the resist etching rate on resist areas exposed to e-beam and that on unexposed resist areas using the etching equipment. General etching conditions for oxidation film etching were used. The assessment sample was the same as that used for the TOF-SIMS and FTIR observation/analysis. It was an Si wafer that was subjected to the application of BARC and acrylic ArF resist and was not patterned. Using an e-beam defect inspection equipment, the resist surface was exposed to e-beam. The e-beam exposure condition is represented by a landing energy of 1500 eV and a scan averaging number of 16. Figure 9 shows how the resist etching rate varies with the depth, as a comparison between e-beam exposed areas and unexposed areas. This figure indicates that the etching rate near the resist surface, more accurately at a depth of about 30 nm from the surface, is lower on the exposed areas than on the unexposed area. Since protective groups are eliminated in the vicinity of the resist surface, it was expected that the etching rate would increase. However, what actually occurred was opposite to this expectation.

It is known that when a DC bias is applied to the upper electrode of an etching equipment, e-beam injection onto the resist surface is promoted during etching to cause the resist surface to become amorphous [9]. Based on this knowledge, we can assume that the etching rate reduction observed this time is due to an amorphousized top resist surface that results from e-beam exposure by an e-beam defect inspection equipment and leads to etching resistance improvement.

The above results concludes that the etching resistance does not deteriorate. However, since it is necessary to minimize CD variations, the e-beam imaging conditions should be set to lower than 1800eV landing energy and avoid using scan average numbers above the required level.

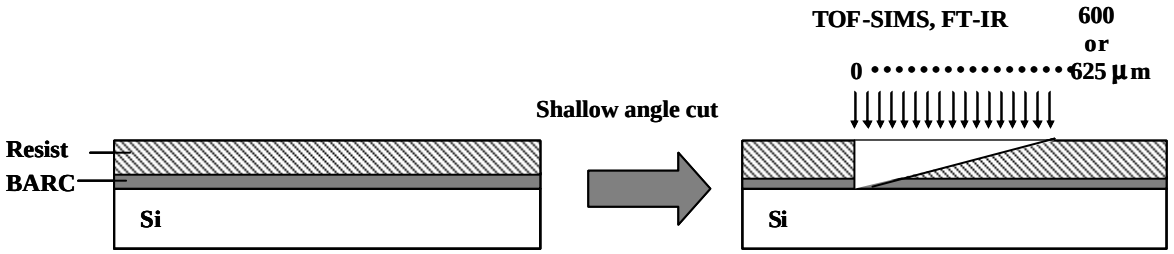

Fig.3 Schematic diagrams of gradient shaving preparation method

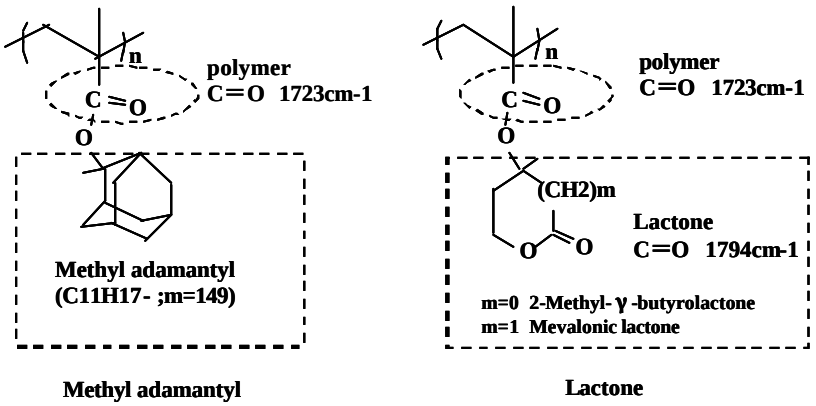

Fig.4 Structure of ArF photo resist for TOF-SIMS and FT-IR analysis

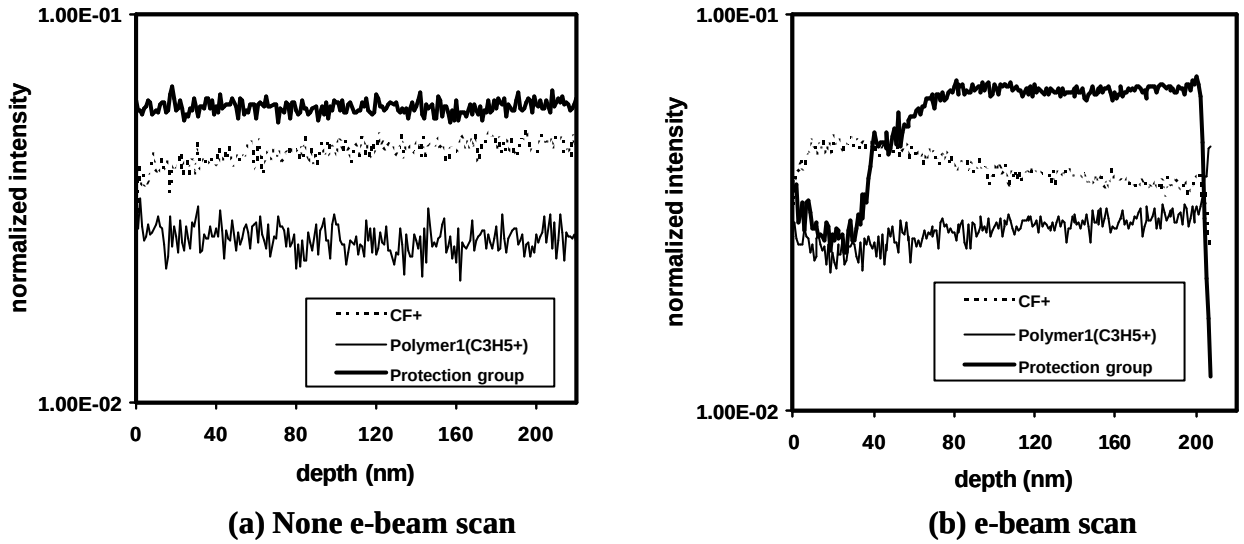

Fig.5 Fragment mass depth distributions of the ArF resist by TOF-SIMS analysis (a)None e-beam scan. (b) e-beam scan

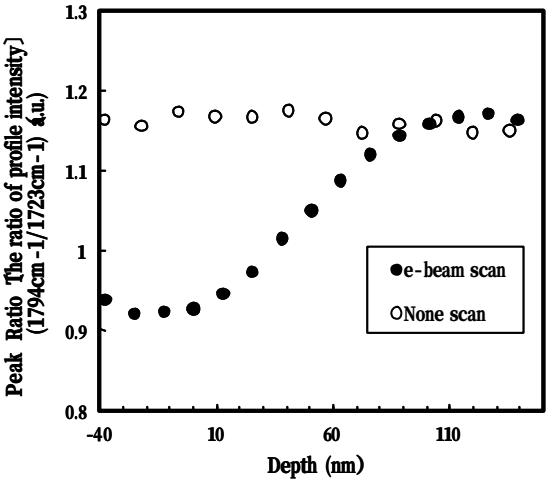

Fig.6 Depth distribution of the peak ratio (C=O bond) by FT-IR

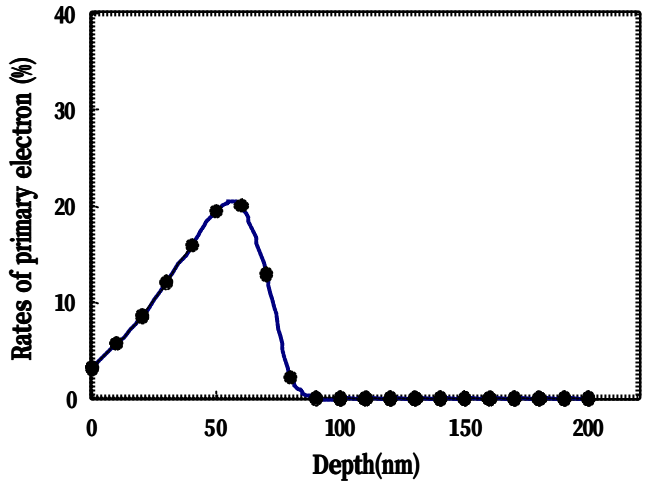

Fig. 7 Calculated penetration depth of primary electron by Monte Carlo simulation in PR

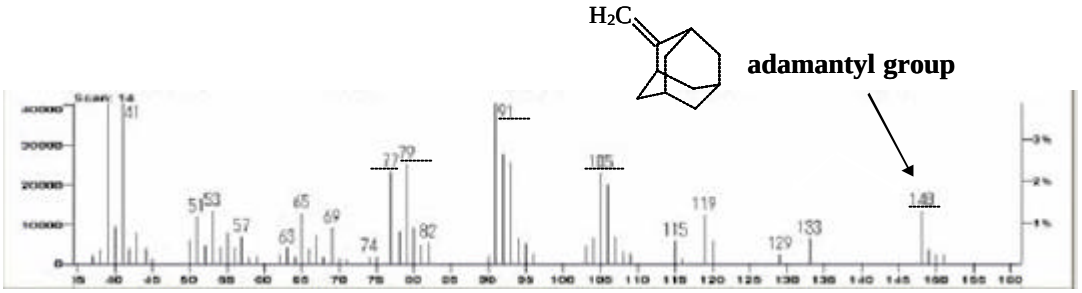

Fig.8 Mass fragment chart of ArF resist and BARC by e-beam radiation

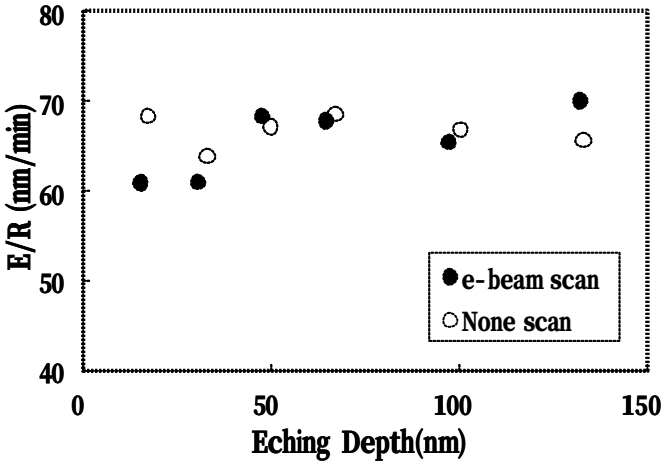

Fig.9 Depth distribution of etching rate in PR

4. PERFORMANCE OF DETECTING 15-nm DEFECTS

Based on the above experimental results, we used an e-beam defect inspection equipment to inspect arrays of programmed defects in a wafer that was patterned with an ArF resist. The inspection was run using conditions that would incur low damage to the resist, and the purpose is to assess its capture rate on such a wafer. Figure 10 shows the structure of the sample. The cross-sectional structure of the sample is as follows: An Si wafer is coated with a thermal oxidation film and a poly-Si film, and then is subjected to the application of BARC and ArF resist to form a line-space structure with a pitch width of 140 nm and a line width of 65 nm. There were 56 programmed defects that were equally spaced in a grid spanning 100 μm x 100 μm area in a 20 mm x 20 mm die. They were 15 to 20-nm extrusion defects created on 65-nm lines. We varied the inspection conditions (i.e. landing energy and scan averages), and compared the defect capture rate under each condition. For each condition, two dies were inspected. Figure 11 shows the results. In this figure, the inspection condition is 1400eV landing energy and 4 scan averages. The figure demonstrates that programmed defects can be detected with high efficiency. It also indicates that inspection can be conducted with very few nuisances. Figure 12 shows how the programmed-defect capture rate depends on the landing energy. The capture rate could be considerably increased when the landing energy exceeds 1200 eV. In addition, the capture rate could be improved when the number of scan averages is 2 or larger.

Based on the above findings, we can conclude that the15 to 20nm programmed extrusion defects on a 65-nm wide line-space structure can be detected at a capture rate of at least 95% and a nuisance rate of up to 5%.

A defect inspection method that features extremely high resolution and low damage has thus been achieved. This method has proved that e-beam defect inspection equipment are of great help to inspect defects on resist wafers with patterns of the 32-nm and later generations.

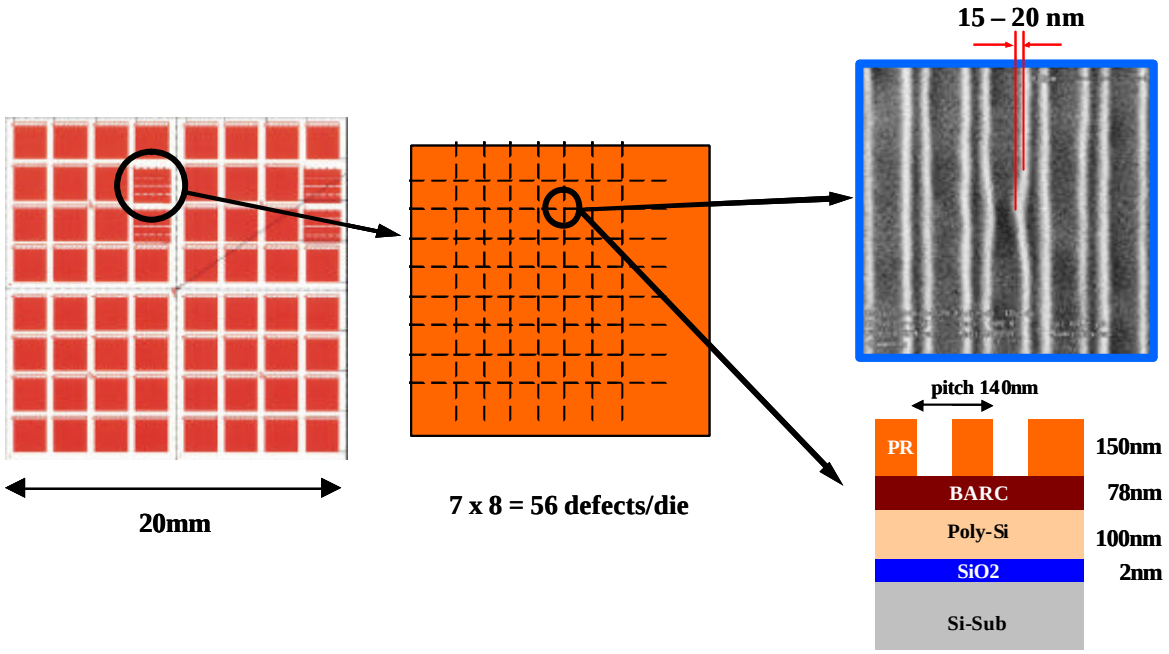

Fig.10 Structure and design of the programmed defect sample

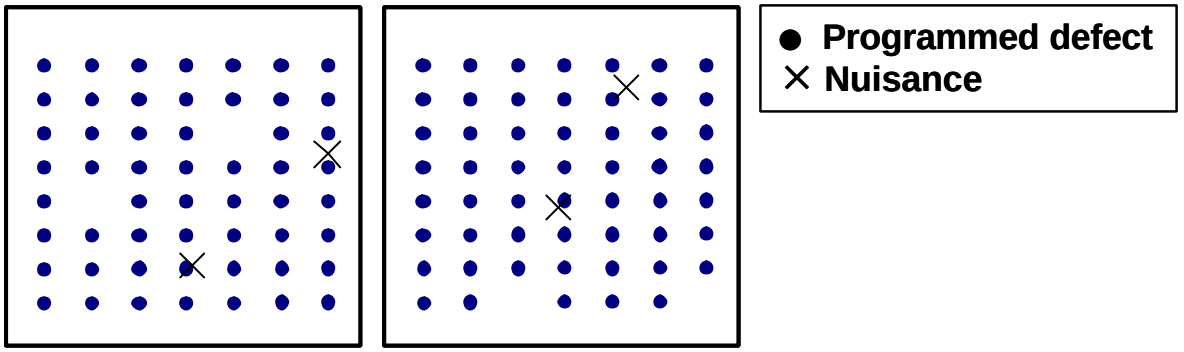

Fig.11 Result of programmed defect inspection

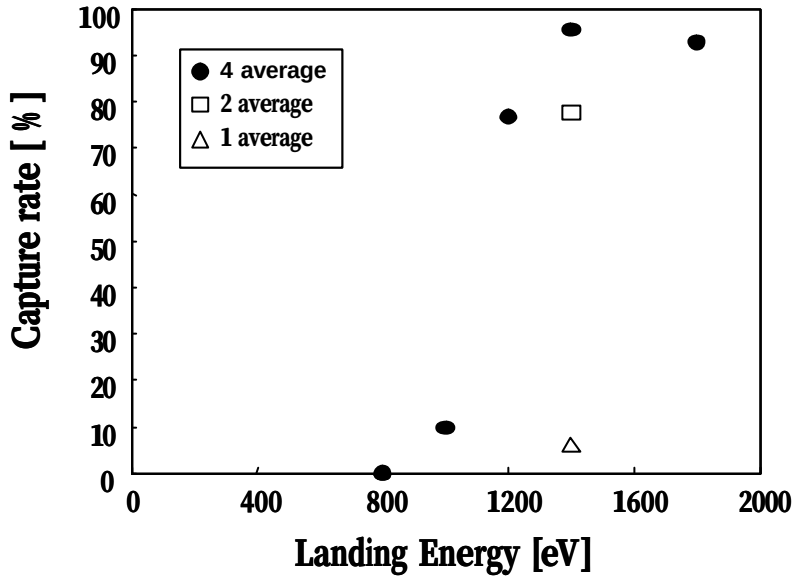

Fig.12 The landing energy dependency of capture rate of programmed defects

5. CONCLUSION

According to the ITRS, the defect size that needs to be controlled at the technology node of the hp 32-nm generation is 16 nm. In this circumstance, optical defect inspection equipment, which are currently in the mainstream, are believed to be no longer adequate for detecting such minute defects. We have therefore verified the usefulness of e-beam defect inspection that features good resolution.

When inspection was conducted using an ebeam defect inspection equipment, it was verified that the CD variations of a 65-nm wide line structure formed with an ArF resist were equal to or less than the CD variations due to a general CD-SEM. The CD variations observed this time were 3% or less on a line width of 65 nm.

We also succeeded in understanding the resist deterioration mechanism that is active when the ArF resist is exposed to e-beam. It has been revealed that the adamantyl group and lactone, which form side chains of the resist, were eliminated in the depth range from the resist surface to the primary electron penetration depth that was calculated by a Monte Carlo simulation. Since the adamantyl group, which is a protective group that helps improve the etching resistance near the surface, was eliminated, it was expected that the etching rate would

increase. We conducted general etching, oxidation film etching, on a resist that was exposed to e-beam. The result indicated that the etching rate was reduced and the etching resistance increased.
Information on inspection conditions that will incur low damage to resists has thus been obtained. Using these inspection conditions, we inspected programmed defects, which were 15 to 20-nm extrusion defects on a line/space structure with a pitch of 140 nm and a line width of 65 nm formed with an ArF resist, using an e-beam defect inspection equipment. These defects were detected at a capture rate of at least 95% and a nuisance rate of 5% or less.
These findings have proved that e-beam defect inspection equipment are useful for inspecting defects on resist wafers with patterns of the 32-nm and later generations.

ACKNOWLEDGEMENT

The authors would like to thank Professor Kaoru Ohya, University of Tokushima for calculation of Monte Carlo simulation.

REFERENCES

1. Jack Jau, et al, "A Novel Method for In-line process Monitoring by Measuring Gray Level Values of SEM images", Proceedings of ISSM, September 2005,pp143-146.
2. X. Liu, et al, "Low energy large scan field electron beam column for wafer inspection", Journal of Vacuum Science& Technology B, Volume 22, Number 6, pp. 3534-3538.
3. Samantha L.Doan, "Expanding the Role of E-beam Inspection in Sub-130nm Flash Memory Development", Proceeding of ISSM, September 2004,pp464-467.
4. M.Saito,et al, "Study of ADI (After Develop Inspection) Using Electron Beam", Proc. of SPIE,vol.6152,615248,2007.
5. A.Habermas, et al, "193nm CD shrinkage under SEM:modeling the mechanism", Proc. of SPIE,vol.4689,pp92-101,2002.
6. T.Kudo, et al, "CD Changes OF 193nm Resists During SEM Mesurement", Proc. of SPIE, vol.4345,pp179-189,2001
7. Tae-Jun You, et al, "CD Metrology for Avoiding Shrinkage of ArF Resist Patterns in 100nm ArF Lithography", Proc. of SPIE, vol.4689,pp724-732,2002.
8. C.H.J.Wu, et al, "Investigation on the Mechanism of the 193nm Resist Linewidth Reduction During the SEM Measurement", Proc. of SPIE, vol.4345, pp190-199,2001.
9. A.Koshiishi," The Equipment Technology and the Concept which is Required as the Oxidation Film Etcher beyond 32-nm Generation Node", Session3 Multi-Level Interconnection & Etching, SEMI Technology Symposium (STS) 2006, SEMICON Japan 2006